

# Control of microstructure of Fe–B microcrystalline materials

LIN YIJIAN

Test Center, Shanghai Iron and Steel Research Institute, 1001 Taihe Road, Wusong, Shanghai, People's Republic of China

The correlations between hardness, microstructure and heat-treatment condition of Fe–B microcrystalline materials were systematically investigated. The means of controlling microstructure by adjusting composition and, thus, the type of boride was also explored. It was established that the grain size of the matrix phase was determined by the volume fraction of dispersive boride particles, and their size follows the formula:  $D_{\max} = 4/3 \bar{r}/f$ , and, in turn determines hardness which obeys the Hall–Petch relation:  $H_v = H_0 + kd^{-1/2}$ . It was also found that the size of the boride particles increases exponentially with increasing temperature and linearly with the fourth root of holding time.  $M_3B_2$  has a lower coarsening rate than  $M_2B$ ; therefore, promoting  $M_3B_2$  and inhibiting  $M_2B$  is an effective measure to stabilize the microcrystalline structure under hot exposure.

## 1. Introduction

Microcrystalline materials, as developed originally by Ray *et al.* [1], possess high strength and other excellent properties owing to the formation of an aggregate structure of ultrafine matrix grains with uniformly dispersed second-phase particles. This unique microstructure is obtained by rapid solidification and proper subsequent heat treatment. The ribbons or powders obtained by rapid solidification must be consolidated at high temperature by conventional powder metallurgy (PM) technology to turn them into bulk materials. An important problem is whether the ultrafine microstructure can be retained in the high-temperature process. For this reason, there is a great need to understand the structural coarsening behaviour of microcrystalline materials at high temperature.

We have reported previously [2] the formation and transformation of borides during melt-quenching and subsequent annealing of an Fe–B microcrystalline alloy ( $Fe_{70}Cr_{18}Mo_2SiB_9$ ). The ribbons melt-spun under a cooling rate of the order of  $10^5 K s^{-1}$  have a cellular microstructure with  $\alpha$ -Fe as cores and  $\alpha$ -Fe- $o$ - $Fe_3B$  eutectic between the cores. After a 300–700 °C anneal  $o$ - $Fe_3B$  disappears and  $Fe_2B$  appears in the form of networks within and between the cells. After annealing at 800–1150 °C, granular  $Cr_2B$  and  $Mo_{1+x}(Fe, Cr)_{2-x}B_2$  are formed. The sizes of the  $\alpha$ -Fe grains and the boride particles rapidly increase with increasing annealing temperature and reach a size of about 1  $\mu m$  after annealing at 1000 °C for 0.5 h. Hardness changes correspondingly with annealing temperature, as shown in Fig. 1. It can be seen that hardness rapidly decreases with microstructural coarsening, indicating a strong effect of structural refinement on strength. Therefore, the present work aimed to study structural coarsening of Fe–B microcrystalline materials under hot exposure and its effect on hardness.

## 2. Experimental procedure

The composition of the test material was  $Fe_{64.2}Cr_{18}Mo_5SiB_{11}Nb_{0.3}Ti_{0.5}$  (at %), a modification to the earlier  $Fe_{70}Cr_{18}Mo_2SiB_9$ , with increased boron to facilitate the formation of the amorphous state in melt-quenching and with an increased molybdenum content and small amounts of niobium and titanium added to promote  $M_3B_2$  [2, 3]. About 60  $\mu m$  thick ribbons were prepared by single-roll melt-quenching, and then subjected to different heat treatments in argon as follows:

- (1) Isochronal anneals each for 0.5 h between 500 and 1100 °C, in steps of 100 °C;
- (2) Isothermal anneals for 0.5, 2 or 8 h at 800 °C and for 0.5, 2 or 4 h at 900 °C;
- (3) Two-stage anneal in the range 600–1000 °C for 0.5 h and 1000 °C for 1 h.

On the quenched and differently annealed ribbons, X-ray diffraction was carried out to analyse phase constitution, and TEM observation was made to study the change of microstructure. Statistics of the sizes of boride particles and matrix grains were derived from the transmission electron micrographs. Hardness tests were performed on the ribbon surface with a load of 9.8 N. In order to ensure the reliability of the test on thin ribbons, we carefully examined by varying the testing loads how the hardness of the sustaining substrate influenced the testing results under different ratios of depth of indentation to thickness of tested foil, and found that testing data remained close to the expected value until the ratio reached 50% if the hardness of the substrate was much higher than that of the samples; that is, the substrate was almost uninvolved with the plastic deformation of the tested sample during the indentation process. Therefore, a much harder substrate was chosen for the hardness tests of the ribbons.

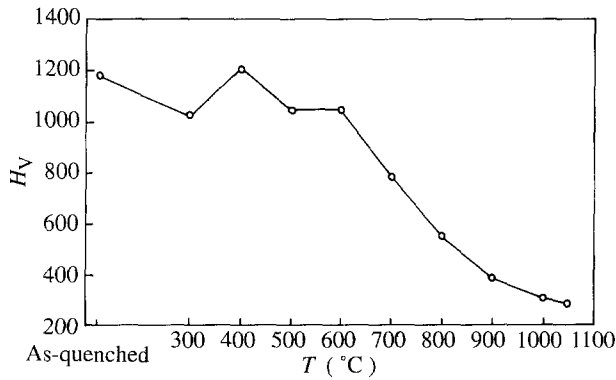


Figure 1 Hardness versus annealing temperature (holding time = 0.5 h) for  $\text{Fe}_{70}\text{Cr}_{18}\text{Mo}_2\text{SiB}_9$  ribbons.

### 3. Results and discussion

X-ray diffraction results are listed in Table I. The quenched ribbons are amorphous except for a very thin surface layer. 500 °C/0.5 h annealed ribbons have not yet crystallized. In 600–700 °C/0.5 h annealed ribbons, apart from  $\alpha\text{-Fe}$ , two metastable phases are formed, one is  $t\text{-M}_3\text{B}$ ; the other, having  $d$  values of 0.2348, 0.2199, 0.1975, 0.1796, 0.1726, 0.1638 nm, has not been identified. The unknown phase, less stable than  $t\text{-M}_3\text{B}$ , decreases from 600–700 °C and  $t\text{-M}_3\text{B}$  increases correspondingly. After annealing at or above 800 °C, a stable phase constitution is formed: apart from the  $\alpha\text{-Fe}$  matrix, there are borides,  $\text{M}_3\text{B}_2$  and  $\text{M}_2\text{B}$ ,  $\text{M}_3\text{B}_2$  being dominant. This phase constitution remains stable up to the highest annealing temperature studied (1100 °C) with the relative amount of each phase basically unchanged. Differential thermal analysis on quenched ribbons (heating rate 20 °C  $\text{min}^{-1}$ ) indicates the main crystallization peak at 626 °C.

TEM reveals that the microstructure of the ribbons annealed at or about 800 °C is featured by uniform aggregates of  $\alpha\text{-Fe}$  grains (white contrast in Fig. 2) with boride particles on a submicrometre scale, which coarsens sensitively with increasing temperature. In Fig. 2, the majority of boride particles showing dark black contrast are  $\text{M}_3\text{B}_2$ , the rest (containing stacking faults and growing faster) are  $\text{M}_2\text{B}$ . The statistical results on the sizes of boride particles and  $\alpha\text{-Fe}$  grains are shown in Tables II and III.

Data analysis indicates that the diameter ( $\bar{d}$ ,  $\mu\text{m}$ ) of the boride particles increases exponentially with increasing temperature ( $T$ , °C) for the same holding time of 0.5 h (Fig. 3), which can be expressed as  $\bar{d} = a \exp(bT)$ . For  $\text{M}_3\text{B}_2$ ,  $a = 1.7 \times 10^{-3}$ ,  $b = 4.8 \times 10^{-3}$ , and for  $\text{M}_2\text{B}$ ,  $a = 1.6 \times 10^{-3}$ ,  $b = 5.5 \times 10^{-3}$ . The coarsening rate is somewhat lower for  $\text{M}_3\text{B}_2$ .

The diameter of the boride particles also increases with prolonged holding time in isothermal annealing, but much more sluggishly compared with its change with temperature. On annealing at 800 °C, the average diameter of  $\text{M}_3\text{B}_2$  increased by only 30% (from 0.084  $\mu\text{m}$  to 0.11  $\mu\text{m}$ ) as the holding time was prolonged 16 times (from 0.5 h to 8 h). Data analysis, as shown in Fig. 4, indicates that the average diameter of boride particles increases linearly with the fourth root of the holding time,  $t$ . According to Ostwald ripening theory,

TABLE I Phase analysis by X-ray diffraction on  $\text{Fe}_{64.2}\text{Cr}_{18}\text{Mo}_5\text{SiB}_{11}\text{Nb}_{0.3}\text{Ti}_{0.5}$  ribbons

Annealing conditions	Phase constitution
As-quenched	Amorphous
500 °C/0.5 h	Amorphous
600 °C/0.5 h	$\alpha\text{-Fe} + t\text{-M}_3\text{B} + \text{unknown phase}$
700 °C/0.5 h	$\alpha\text{-Fe} + t\text{-M}_3\text{B} + \text{unknown phase}$
800 °C/0.5 h	$\alpha\text{-Fe} + \text{M}_3\text{B}_2 + \text{M}_2\text{B}$
900 °C/0.5 h	$\alpha\text{-Fe} + \text{M}_3\text{B}_2 + \text{M}_2\text{B}$
1000 °C/0.5 h	$\alpha\text{-Fe} + \text{M}_3\text{B}_2 + \text{M}_2\text{B}$
1100 °C/0.5 h	$\alpha\text{-Fe} + \text{M}_3\text{B}_2 + \text{M}_2\text{B}$

TABLE II Variation of sizes of grains and boride particles with annealing temperature

	Size ( $\mu\text{m}$ )			
	800 °C/ 0.5 h	900 °C/ 0.5 h	1000 °C/ 0.5 h	1100 °C/ 0.5 h
$\text{M}_3\text{B}_2(\bar{d}_1)$	0.084	0.12	0.21	0.34
$\text{M}_2\text{B}(\bar{d}_2)$	0.13	0.22	0.38	0.73
$\alpha\text{-Fe}$	$D_{\text{max}}$	0.27	0.38	0.74
	$\bar{D}$	0.165	0.23	0.46

there should be a  $\bar{d}\text{-}t^{1/3}$  linear relationship in the particle coarsening process if the process is controlled by bulk diffusion. However, for the particles located at grain boundaries, coarsening is controlled by grain-boundary diffusion; in this case, their size increases linearly with  $t^{1/4}$  instead of  $t^{1/3}$  [4]. Because devitrification occurs at a temperature much higher than the crystallization temperature, the nucleation rate is very high, leading to instant formation of a homogeneous aggregate of boride particles and matrix grains on an ultrafine scale. Consequently, the subsequent particle coarsening process is controlled by grain-boundary diffusion. The co-existence of the two kinds of borides does not cause obvious disturbance to their coarsening pattern, probably because the coarsening of  $\text{M}_2\text{B}$  and  $\text{M}_3\text{B}_2$  is controlled, respectively, by diffusion of chromium and molybdenum atoms [2].

The matrix grain size is determined by the volume fraction of dispersed boride particle and their sizes. The test data are found to be in agreement with the Zener formula  $D_{\text{max}} = 4/3 \bar{r}/F$  [5], where  $D_{\text{max}}$  is the maximum diameter of matrix grains, usually  $D_{\text{max}}/\bar{D} = 1.6\text{--}1.8$  in the present work,  $F$  is the volume fraction of boride, which is estimated to be about 20% and  $\bar{r}$  is the average radius of boride particles. The data show that if  $\bar{r}$  is taken as the average radius of the dominant boride  $\text{M}_3\text{B}_2$ , then in the high-temperature range of above 1000 °C only, the measured grain is a little larger than that predicted by this formula due to the fast coarsening of  $\text{M}_2\text{B}$  particles. As a result, the grain size of the matrix also increases exponentially with increasing temperature and linearly with  $t^{1/4}$ .

The two-stage annealing test indicates that the ribbons first annealed for 0.5 h at different temperatures from 600–1000 °C and then subjected to a second anneal together at 1000 °C for 1 h, have nearly the same microstructure, although the first-stage anneal

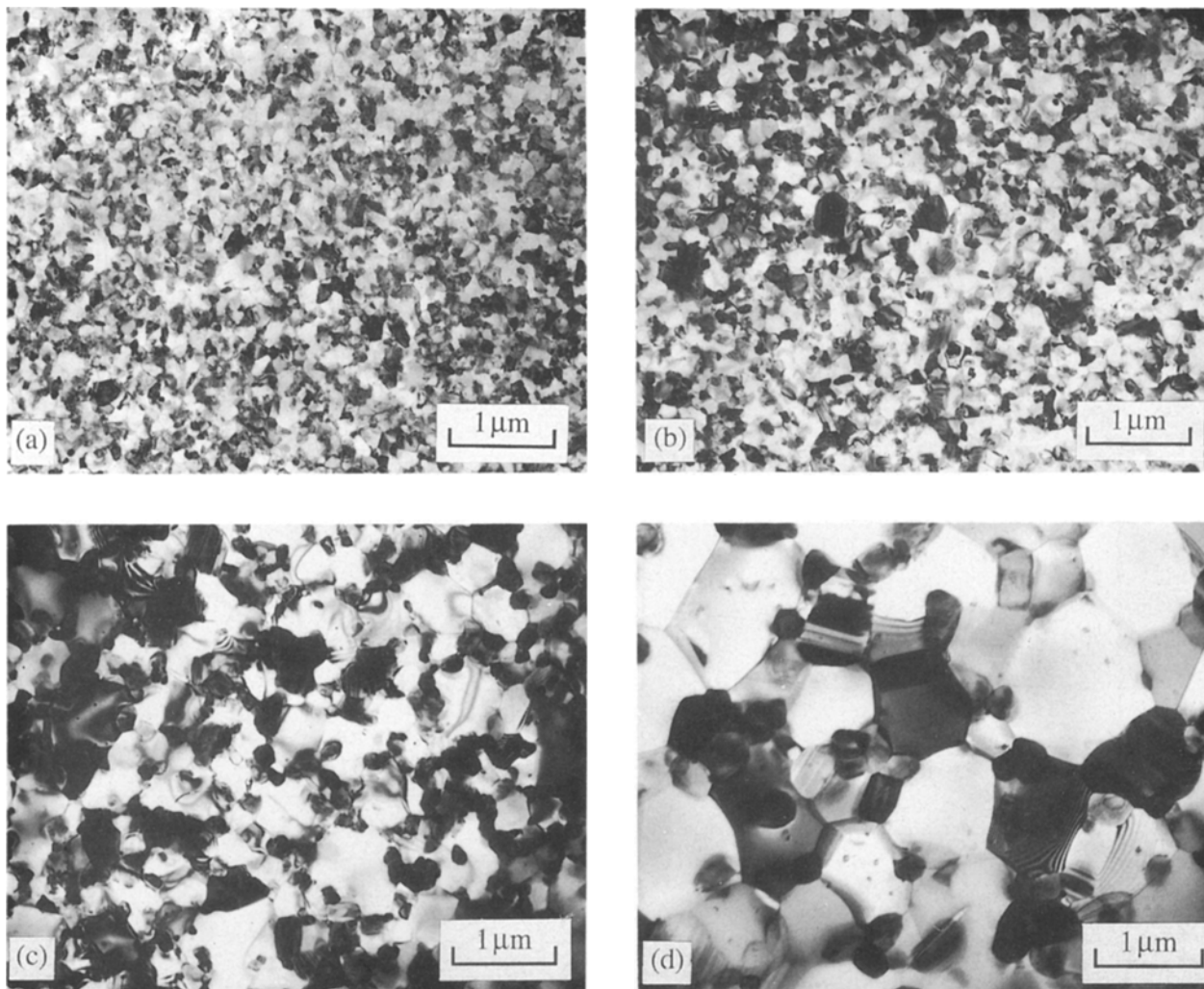


Figure 2 Devitrification microstructure of  $\text{Fe}_{64.2}\text{Cr}_{18}\text{Mo}_5\text{SiB}_{11}\text{Nb}_{0.3}\text{Ti}_{0.5}$ , annealed at (a)  $800\text{ }^\circ\text{C}/0.5\text{ h}$ , (b)  $900\text{ }^\circ\text{C}/0.5\text{ h}$ , (c)  $1000\text{ }^\circ\text{C}/0.5\text{ h}$ , and (d)  $1100\text{ }^\circ\text{C}/0.5\text{ h}$ .

TABLE III Variation of sizes of grains and boride particles with annealing time

	Size ( $\mu\text{m}$ )					
	$800\text{ }^\circ\text{C}/0.5\text{ h}$	$800\text{ }^\circ\text{C}/2\text{ h}$	$800\text{ }^\circ\text{C}/8\text{ h}$	$900\text{ }^\circ\text{C}/0.5\text{ h}$	$900\text{ }^\circ\text{C}/2\text{ h}$	$900\text{ }^\circ\text{C}/4\text{ h}$
$\text{M}_3\text{B}_2 (\bar{d}_1)$	0.084	0.10	0.11	0.12	0.14	0.15
$\text{M}_2\text{B}(\bar{d}_2)$	0.13	0.16	0.18	0.22	0.31	0.36
$\alpha\text{-Fe}(\bar{D})$	0.165	0.18	0.195	0.23	0.275	0.30

causes obvious differences in structural refinement or even in phase constitution. The microstructure of the two-stage annealed ribbons is also similar to that of the ribbon subjected to a single anneal to  $1000\text{ }^\circ\text{C}$ . This suggests that the final microstructure is basically determined by the maximum temperature stage of the whole heat-treatment process and is hardly influenced by the early treatment at lower temperatures.

Hardness changes as a function of annealing conditions in the same way as the degree of structural refinement, being very sensitive to annealing temperature and less influenced by holding time. Fig. 5 shows the change of hardness with temperature in 0.5 h isochronal annealing. Hardness increases as crystallization takes place and metastable phases form during  $600\text{--}700\text{ }^\circ\text{C}$  annealing, and decreases as stable phase constitution forms and structural coarsening

proceeds on annealing above  $800\text{ }^\circ\text{C}$ . Ribbons annealed at  $500\text{--}700\text{ }^\circ\text{C}$  become very brittle so that cracks occur along indentation in hardness test under a load of 9.8 N. The hardness values are shown in Fig. 5 for these conditions obtained under a load of 4.9 N. The brittleness of the  $500\text{ }^\circ\text{C}$  annealed ribbon, which has not yet crystallized, must be related to structural relaxation of the amorphous state, and may be useful for pulverization of ribbons for PM technology. After the stable phase constitution is formed, ribbons show some ductility and their ductility increases with decreasing hardness.

Fig. 6 shows the change of hardness with holding time in the isothermal annealing. It can be seen that the change of hardness becomes sluggish with prolonged holding time, corresponding to a  $\bar{d}\text{-}t^{1/4}$  relation.

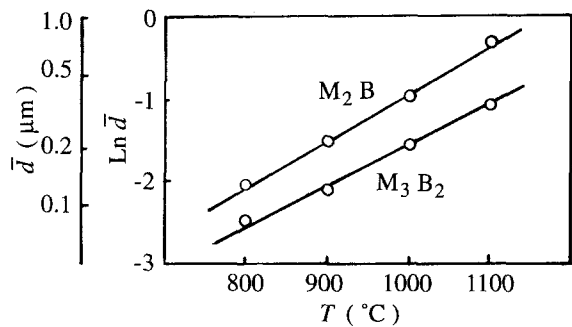


Figure 3 Variation of boride size with annealing temperature (holding time = 0.5 h).

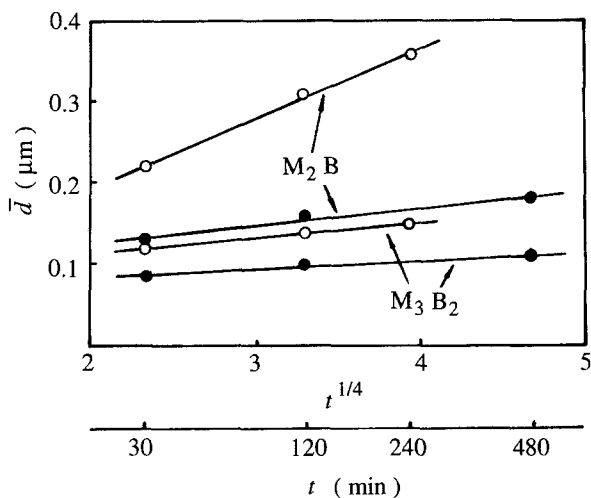


Figure 4 Variation of boride size with annealing time, at (—●—) 800°C, and (—○—) 900°C.

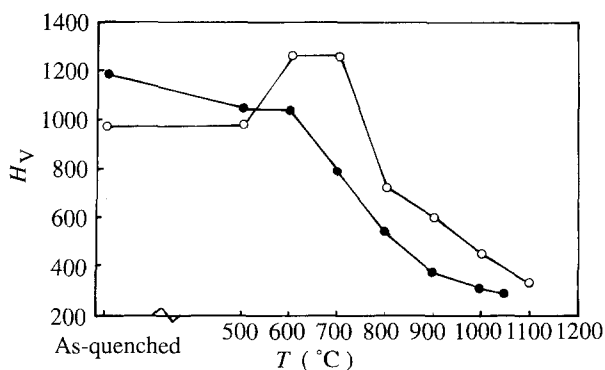


Figure 5 Variation of hardness with annealing temperature (holding time = 0.5 h) for  $\text{Fe}_{64.2}\text{Cr}_{18}\text{Mo}_5\text{SiB}_{11}\text{Nb}_{0.3}\text{Ti}_{0.5}$  ribbons (—○—) compared with  $\text{Fe}_{70}\text{Cr}_{18}\text{Mo}_2\text{SiB}_9$  ribbons (—●—).

Like its influence on structural refinement, the two-stage annealing leads to nearly the same hardness value after the second-stage anneal at the same temperature of 1000°C, in spite of a big difference in hardness caused by different early anneals at lower temperatures.

By relating the hardness to the corresponding grain size, we found that they obey the Hall–Petch relation;  $H_V = H_0 + Kd^{-1/2}$ , as shown in Fig. 7. It has long been known that there is a Hall–Petch relation between hardness and grain size for many metallic materials [6], the reported test range of grain size being usually larger than 1  $\mu\text{m}$ . The present result, indicates

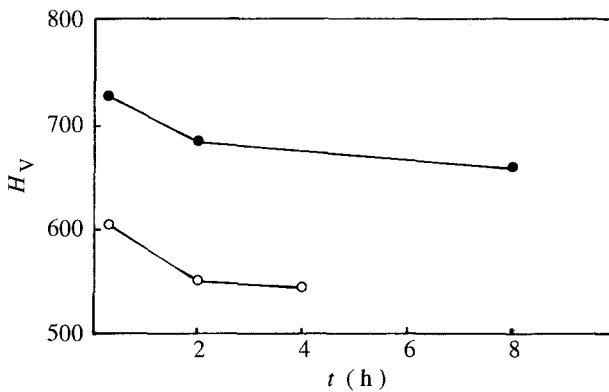


Figure 6 Variation of hardness with annealing time at (—●—) 800°C, and (—○—) 900°C.

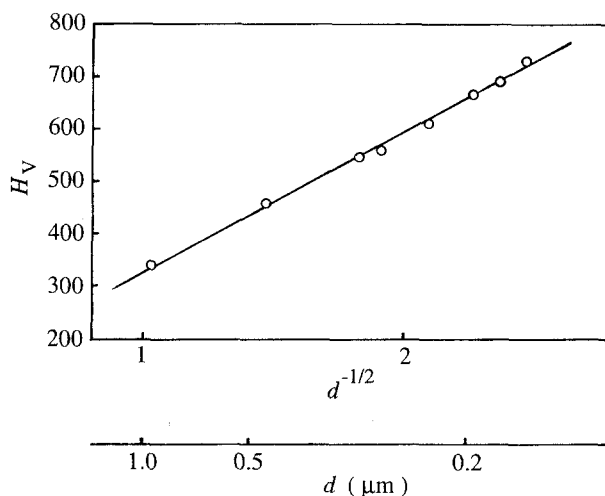


Figure 7 Variation of hardness with grain size of  $\alpha\text{-Fe}$  matrix.

that the Hall–Petch relation is still valid for submicrometre grain sizes, showing great potentialities in high strength for microcrystalline materials.

Compared with Fig. 1, Fig. 5 shows an obvious increase in hardness of the ribbons for the testing composition over the original composition. Correspondingly, for the bulk materials produced from the ribbons through 950°C/2.5 h hot isostatic pressing, the testing composition is superior to the original composition both in room-temperature hardness and hot hardness, as shown in Table IV (in this test, load = 98 N, load time = 45s). The reasons for the superiority of the testing material over the original one can be determined from a study of their microstructures (compare Fig. 2 with Fig. 4 in [2]) as follows.

(1) More uniform microstructure can be obtained by devitrification of the amorphous state, and microsegregation can be avoided. The amorphous state is attained by melt-quenching due to an increased glass-forming tendency by increasing the boron content.

(2) The stability of the ultrafine microstructure is favoured by promoting  $\text{M}_3\text{B}_2$ , which has a lower coarsening rate.  $\text{M}_3\text{B}_2$  is promoted due to increasing or adding  $\text{M}_3\text{B}_2$ -promoting elements such as molybdenum, niobium or titanium.

(3) A higher fraction of boride due to increasing boron content results in more refined matrix grains and, thus, higher hardness, as determined by the formula  $D_{\text{max}} = 4/3\bar{r}/F$ .

TABLE IV Comparison of hardness of bulk materials between testing composition and original composition

	$H_V$					
	RT	300 °C	500 °C	550 °C	600 °C	700 °C
$Fe_{10}Cr_{18}Mo_2SiB_9$	336	272	227	208	169	78.3
$Fe_{64.2}Cr_{18}Mo_5SiB_{11}Nb_{0.3}Ti_{0.5}$	451	381	297	264	236	118

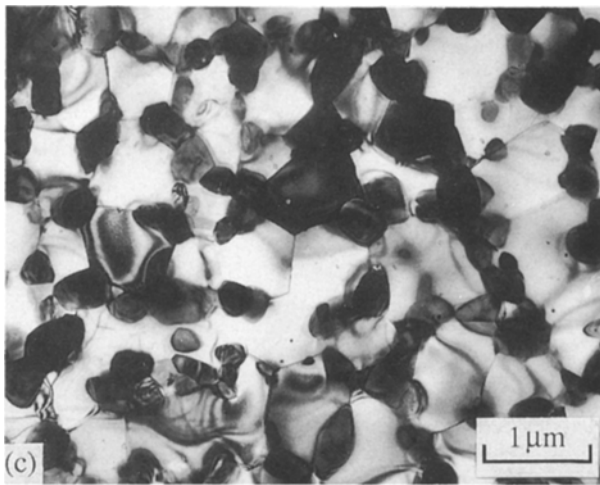
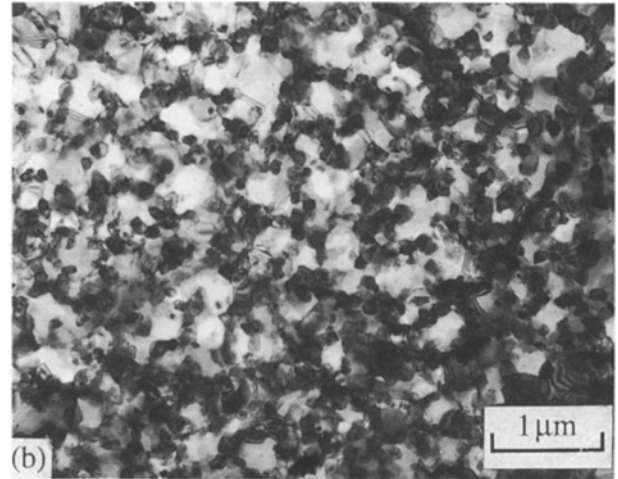
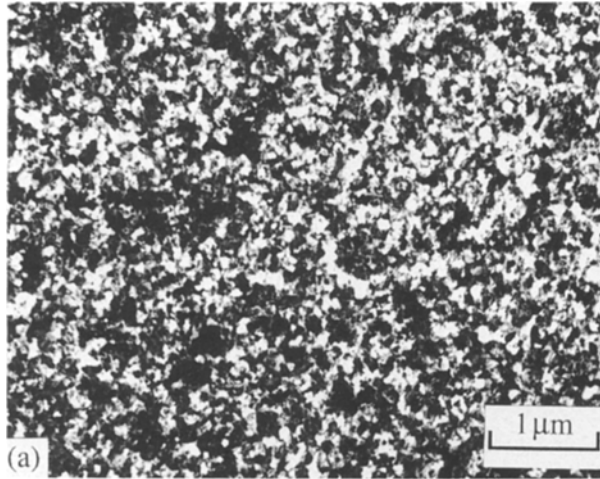


Figure 8. Devitrification microstructure of  $Fe_{57}Cr_{18}Mo_{10}SiB_{13}Nb_{0.5}Ti_{0.5}$  annealed at (a) 900 °C/0.5 h, (b) 1000 °C/0.5 h, and (c) 1100 °C/0.5 h.

TABLE V Comparison of hardness under different annealing conditions between  $Fe_{64.2}Cr_{18}Mo_5SiB_{11}Nb_{0.3}Ti_{0.5}$  and  $Fe_{57}Cr_{18}Mo_{10}SiB_{13}Nb_{0.5}Ti_{0.5}$  ribbons

	$H_V$		
	900 °C/ 0.5 h	1000 °C/ 0.5 h	1100 °C/ 0.5 h
$Fe_{64.2}Cr_{18}Mo_5SiB_{11}Nb_{0.3}Ti_{0.5}$	604	455	338
$Fe_{57}Cr_{18}Mo_{10}SiB_{13}Nb_{0.5}Ti_{0.5}$	665	520	389

It should be pointed out that there is a limit to increasing the boron content. Ray [7] suggested that the total amount of metalloids including boron should not be more than 12 at %. The reason for this is that overmuch boride will cause serious brittleness. We studied the effect of different boron contents on the properties of Fe–B microcrystalline materials [2, 8] and found that the embrittlement results from boride particles overgrowing and contacting with each other, or even forming a continuous rigid frame. Therefore the limit to the increasing boron content should be set at the point at which the boride retains its dispersed morphology of fine particles in the matrix. Under this condition, slightly more boron than the original design can be safely adopted for further increasing strength without losing necessary ductility.

Based on this understanding, we undertook a supplementary experiment on a further modified composition:  $Fe_{57}Cr_{18}Mo_{10}SiB_{13}Nb_{0.5}Ti_{0.5}$  in which the increasing molybdenum amount is to promote  $M_3B_2$

and inhibit,  $M_2B$  and, at the same time, to appropriately increase the boron content in the hope of increasing the volume fraction of dispersive fine  $M_3B_2$  particles. The resultant microstructure is more uniform and more refined, as shown in Fig. 8 (cf. Fig. 2).

Nearly all the boride particles are of  $M_3B_2$ , homogeneously distributed, being smaller than 1 μm even after 1100 °C/0.5 h annealing and mostly located at intersections of grain boundaries, effectively inhibiting grain growth. Correspondingly, an increased hardness ( $H_{V,RT}$ , load 1 kg) is obtained, as shown in Table V, with some ductility retained.

#### 4. Conclusion

The correlation between hardness, microstructure and heat-treatment conditions of Fe–B microcrystalline materials was systematically investigated. The following results were obtained.

1. The grain size of the matrix is determined by volume fraction and particle size of the borides

contained in the alloys, following the Zener formula  $D_{\max} = 4/3\bar{r}/F$ . Whether the microcrystalline structure can be retained in the process of heat treatment, depends on the thermo-size stability of boride particles under hot exposure.

2. Structural coarsening is very sensitive to temperature but less influenced by holding time in heat treatment. In isochronal annealing, the diameters of the grains and boride particles increase exponentially with increasing temperature. In isothermal annealing, the diameters of the grains and boride particles increase with holding time, exhibiting a linear relationship between  $\bar{d}$  and  $t^{1/4}$ . In two-stage annealing, the final microstructure is determined by the highest temperature stage of the whole process.

3. Hardness tested at room temperature relates to the matrix grain size in agreement with the Hall-Petch relation,  $H_v = H_0 + Kd^{-1/2}$ , in the sub-micrometre range of grain size. This indicates great potentialities in high strength for microcrystalline materials.

4.  $M_3B_2$  has a lower coarsening rate compared to  $M_2B$ . Therefore promoting  $M_3B_2$  and inhibiting  $M_2B$

by increasing  $M_3B_2$ -promoting elements can effectively increase the stability of ultrafine microstructure under hot exposure.

## References

1. R. RAY, V. PANCHANATHAN and S. ISSEROW, *J. Metals* **35**(6) (1983) 30.
2. LIN YIJIAN and HU JIAN, *J. Mater. Sci.* **26** (1991) 2833.
3. HU JIAN, Master's Degree Thesis, Shanghai Iron and Steel Institute (1987).
4. A. J. ARDELL, *Acta Metall.* **20** (1972) 601.
5. E. P. ABRAHAMSON, in "Ultrafine-Grain Metals", edited by J. J. BURKE and V. Weiss (Syracuse University Press, New York, 1971).
6. R. M. DOUTHWAITE, *J. Iron Steel Inst.* **208** (1970) 265.
7. R. RAY, in "Rapidly Solidified Amorphous and Crystalline Alloys", edited by B. H. Kear, B. C. Giessen and M. Cohen (Elsevier Science, New York, 1982) p. 435.
8. Y. LIN, Y. YOU, C. JING and Q. YU, *J. Iron Steel Res.* **2**(2) (1990) 55 (in Chinese).

*Received 4 March*

*and accepted 27 April 1993*